Immersion and dry lithography monitoring for flash memories (after develop inspection and photo cell monitor) using a darkfield imaging inspector with advanced binning technology

P. Parisi[a], A. Mani[a], C. Perry-Sullivan[a], J. Kopp[a], G. Simpson[a], M. Renis[b], M. Padovani[b], C. Severgnini[b], P. Piacentini[b], P. Piazza[b], A.Beccalli[b]
[a]KLA-Tencor, Corp., 1 Technology Drive, Milpitas, CA 95035 USA;
[b]Numonyx R2 Technology Center, Via C. Olivetti 2, 20041 Agrate Brianza (MI) Italy

ABSTRACT

After-develop inspection (ADI) and photo-cell monitoring (PM) are part of a comprehensive lithography process monitoring strategy. Capturing defects of interest (DOI) in the lithography cell rather than at later process steps shortens the cycle time and allows for wafer re-work, reducing overall cost and improving yield. Low contrast DOI and multiple noise sources make litho inspection challenging. Broadband brightfield inspectors provide the highest sensitivity to litho DOI and are traditionally used for ADI and PM. However, a darkfield imaging inspector has shown sufficient sensitivity to litho DOI, providing a high-throughput option for litho defect monitoring. On the darkfield imaging inspector, a very high sensitivity inspection is used in conjunction with advanced defect binning to detect pattern issues and other DOI and minimize nuisance defects. For ADI, this darkfield inspection methodology enables the separation and tracking of 'color variation' defects that correlate directly to CD variations allowing a high-sampling monitor for focus excursions, thereby reducing scanner re-qualification time. For PM, the darkfield imaging inspector provides sensitivity to critical immersion litho defects at a lower cost-of-ownership. This paper describes litho monitoring methodologies developed and implemented for flash devices for 65nm production and 45nm development using the darkfield imaging inspector.

Keywords: after-develop inspection, photo-cell monitoring, litho monitoring, darkfield inspection

1. INTRODUCTION

After-develop inspection (ADI) and photo-cell monitoring (PM) are part of a comprehensive lithography process monitoring strategy. ADI is performed on product wafers after resist coat, exposure and development. PM is done on test wafers and monitors track and scanner performance. Capturing defects in the litho cell rather than at later process steps shortens the cycle time and allows for wafer re-work, reducing overall cost and improving yield.

Low contrast defects of interest (DOI) and multiple noise sources make litho inspection challenging. Broadband brightfield inspectors with selectable illumination bands and optical apertures provide the highest sensitivity to litho DOI[1]. However, a darkfield imaging inspector with advanced binning capabilities has proven to provide a high-throughput option for litho defect monitoring[2].

This paper describes a methodology that has been developed and implemented in production for monitoring litho layers. On a darkfield imaging inspector, a very high sensitivity inspection is used in conjunction with advanced defect binning to detect pattern issues and other DOI and remove nuisance defects. Starting with 65nm flash ADI, this methodology enables the separation and tracking of 'color variation' defects that correlate directly to CD variations caused by an out-of-focus situation. This unique capability along with the darkfield imaging inspector's high throughput produces a high-sampling monitor for focus excursions and reduces the time required for scanner re-qualification.

For PM, this methodology produces sensitivity to random defects at a lower cost-of-ownership. Based on an extensive study that compared relative capture of critical immersion defects, the darkfield imaging inspector was implemented as tool-of-record for immersion lithography daily photo-cell monitoring.

2. ADVANCED ADI ON DARKFIELD IMAGING INSPECTOR

After-develop inspection (ADI) is used to identify, monitor and reduce pattern defectivity in the lithography cell. ADI is performed on product wafers after resist deposition, exposure and development. Inspection at ADI is challenging

Lithography Asia 2009, edited by Alek C. Chen, Woo-Sung Han, Burn J. Lin, Anthony Yen,
Proc. of SPIE Vol. 7520, 75201W · © 2009 SPIE · CCC code: 0277-786X/09/$18 · doi: 10.1117/12.835839

because the defects are small and low contrast and there are multiple sources of nuisance defects. Nuisance defects at ADI can include: prior-level defects (such as metal grain) that are seen through the transparent top-level resist; color variation resulting from process variations across the wafer; or, resist line roughness. The goal of ADI is to detect yield-critical, pattern defects while minimizing the number of nuisance defects, thereby producing meaningful inspection results that help engineers to quickly identify litho excursions.

While the typical goal of litho inspection is to minimize the detection of 'color variation' nuisance defects, it was discovered at Numonyx that these low signal-to-noise defects on ADI layers can correlate to CD line variations caused by focus excursions. In addition to detecting these CD variations, the Puma 9000 darkfield imaging inspector with automatic defect classification capability was able to separate random physical defects from the 'systematic' CD variations. This defect binning capability allowed a single darkfield imaging inspection to be used for two purposes. First, the random defect bin can be used to monitor general ADI defectivity at nominal focus – helping to identify general process issues. Second, the systematic defect bin can be used to identify focus drift excursions, enabling engineers to re-qualify the scanner before the issue results in device failures due to line shorts, breaks or collapsed structures. In the following discussion, a 'systematic' defect refers to wafer color variation that corresponds to pattern CD variation.

This section presents inspection setup techniques used on a darkfield imaging inspector to detect focus excursions; correlation of the resulting inspection data to spectroscopic CD measurements; and, ADI production data from the darkfield imaging tool demonstrating capture of several excursions related to either CD variations or other litho process issues.

2.1 Darkfield imaging inspection setup and data analysis

An inspection recipe sets the values of the inspector's multiple optical and algorithm parameters. Each parameter is tuned so that when the recipe is run, the DOI are captured at the required nuisance rate. In order to setup a Puma 9000 darkfield imaging inspector recipe capable of detecting and binning systematic CD variations, a set of FEM wafers was produced. The wafer technology was 65nm flash and the process layer was STI photo. Each wafer in this set was exposed at a different focus in order to simulate a production focus excursion. The nine wafers in the set were exposed in the range -120nm to +120nm from the nominal focus in 30nm steps. This exposure range covered the highest tolerable CD variation to the first negative and positive focus offsets that generated collapse of critical structures and produced a noticeable increase in physical defectivity.

The wafer exposed at nominal focus represented a typical production wafer, and was used to setup a standard ADI inspection recipe on the darkfield imaging inspector. This recipe produced good sensitivity to random litho DOI with a SEM Non-Visual (SNV) rate of <10%. This inspection recipe was used to produce the results shown in Figure 1a for the nominal, +60nm and -60nm wafers.

In order to detect the very low signal-to-noise defects related to CD or pattern variations, the defect detection algorithm recipe parameters on the darkfield imaging inspector were adjusted. These parameters were iteratively lowered until the inspection results for the wafers patterned with focus offsets showed clusters of defects related to the stepper field. Inspection results obtained using this high-sensitivity recipe are shown in Figure 1b.

The final step in the inspection recipe setup was to determine the automated defect binning parameters. The resulting defect classification scheme resulted in four different defect bins (Figure 1c): bin 1 – random defects in the circuitry region of the device; bin 2 – random defects in the array region of the device; bin 11 – systematic defects (CD variations) in the circuitry; and, bin 12 – systematic defects in the array. By considering only the defects in bins 1 and 2, as shown in Figure 1d, an inspection result is obtained that contains random litho defects at a nuisance defect rate of <10%. This inspection result is similar in defect density and defect signatures to the result obtained using a standard production recipe (Figure 1a) – not only for the nominal focus wafer, but also for wafers where the focus offset caused a line collapse or failure of critical structures (i.e. wafer map comparison in Figures 1a and 1d for -60nm focus offset wafer). By considering only the defects in bins 11 and 12 (Figure 1e), new information related to CD variations is obtained. Thus, by running the high-sensitivity inspection recipe in conjunction with the automated defect binning scheme, engineers can track random defects for production litho monitoring, and track systematic defects for focus excursion monitoring.

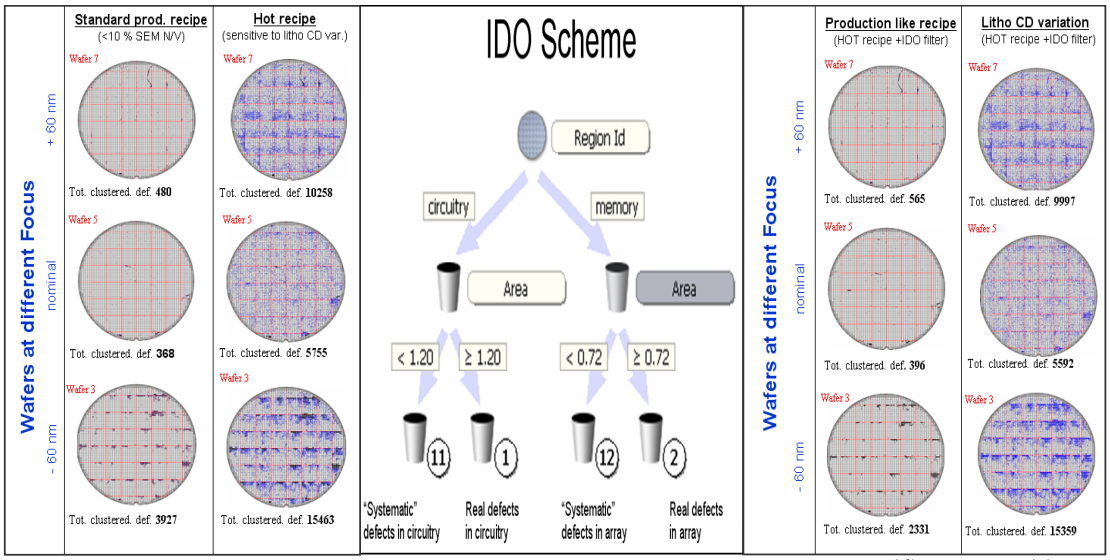

Fig. 1. Inspection results from the Puma 9000 darkfield imaging inspector for three wafers – nominal focus, and +/- 60nm focus offset. Wafer maps in (a) were generated using a standard production recipe. Results in (b) were generated using a high-sensitivity recipe capable of detecting CD variations. The automated defect binning scheme (iDO; inline Defect Organizer feature of the Puma 9000) is shown in (c). Running the high-sensitivity recipe with automated binning produces the results shown in (d) and (e). Only random defects from bins 1 and 2 are shown in (d), while systematic defects from bins 11 and 12 are shown in (e).

All wafers in the focus exposure set were inspected on the darkfield imaging inspector using the high-sensitivity recipe with automated defect binning. The resulting data is shown in Figure 2 with clustered defect count and clustered defect density plotted versus litho focus step for the seven wafers exposed in the range of -90nm to +90nm. The wafers exposed at +/-120nm are not shown in this analysis because they were too defective. For reference, four fields from the center of the defect wafer map are shown for each data point. Clustering was used to reduce multi-hit contribution to defect density from large scratch defects. Overall, pre- and post-clustering defect counts were similar for the systematic defect type.

Systematic defect density (Figure 2a; bins 11 and 12) shows a parabolic behavior with a very sensitive step rise occurring asymmetrically at 30nm for negative focus variation and 60nm for positive focus variation. This defect density increase is visible as stepper field signature and clusters in the sections of the defect wafer maps displayed.

The random defect density (Figure 2b; bins 1 and 2) remains flat and under the production baseline SPC limit for the wafers exposed within the range of -30nm to +60nm. No defect signature or clusters are visible on the wafer maps for the wafers within this focus range. For wafers with a focus offset above +60nm or below -30nm, there is an increase in random defect density. This increase is related to defects that are printed on the wafers because of critical structure collapse caused by litho defocus.

Based on these data, it is possible to define three areas for defect density as a function of focus offset. Within the 'no variation area' (green area of the charts in Figure 2), the random defect density is below SPC limits and the systematic defect density is low with no stepper field defect signatures or clusters. Within the 'CD variation area' (yellow on Figure 2 charts), there is little to no increase in random defect density but the increase in systematic defect density is dramatic and stepper field defect signatures begin to appear on the wafer maps. The 'defect print area' (orange area in Figure 2) is comprised of the focus offsets that cause defects to print on the wafers, resulting in high random and systematic defect density.

These data suggest that it may be possible to set a second SPC limit based on systematic defect density. When both systematic and random defect densities are above their respective SPC limits, then the scanner should be put down for re-qualification. When the random defect density is below its SPC limit and the systematic defect density is above its SPC limit, a warning can be sent to litho engineers and preventative action can be taken before a defocus condition results in printed defects on the wafers.

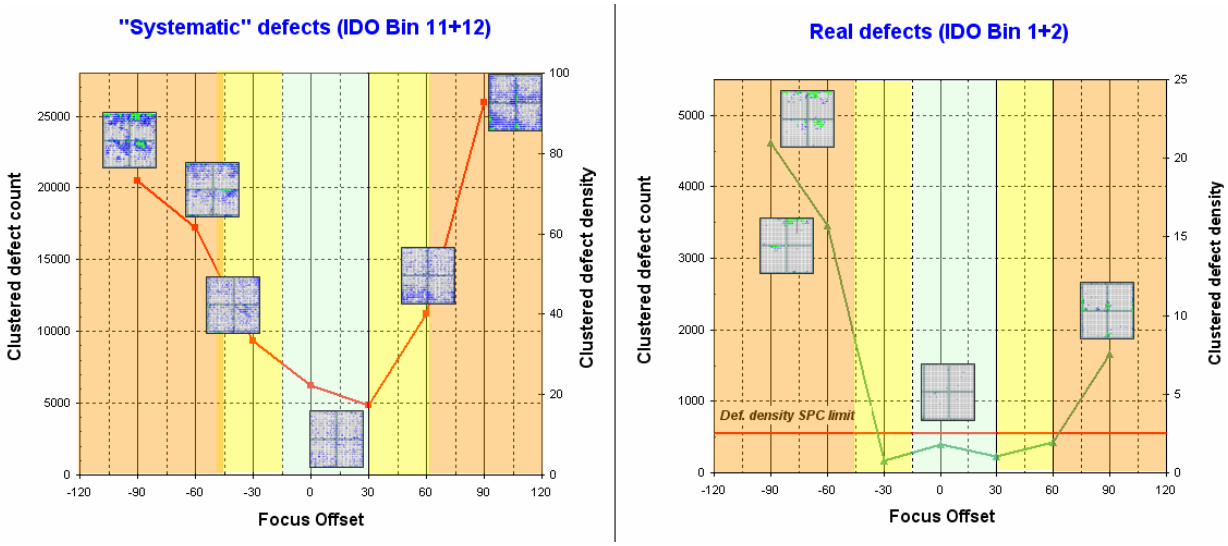

Fig. 2. Clustered defect density plotted versus focus offset for seven wafers in the focus range of -90nm to +90nm. Systematic defect density (bins 11 and 12) is shown in the left-hand graph and random defect density (bins 1 and 2) is shown in the graph on the right.

2.2 Correlation of inspection data and spectroscopic CD measurements

In order to establish correlation between the systematic defect density variations and actual geometric variations in the critical dimensions of printed features, the set of wafers exposed at different focus offsets was inspected on KLA-Tencor's Spectra CD-XT broadband spectroscopic CD (SCD) measurement tool.

The SCD technology is based on a broadband spectroscopic ellipsometer (SE) hardware platform that is used to collect pattern diffraction and refraction signals in the UV-Visible (240 – 750nm) range of the electromagnetic spectrum. The two-dimensional profile reconstruction of the feature to be measured is calculated in real time by comparison between measured signal and a first principle derived model with a library-based numerical fit approach. Inputs for library generation are the optical dispersion properties of the materials constituting the structure and the film stack, the grating pitch, and boundary condition limits for the degrees of freedom building up the parametric model (CD, grating height, sidewall angles, layers thickness). The optical dispersion properties of the materials were modeled from blanket wafers. With reference to the specific geometry of the pattern to reconstruct, all measurements were carried out so that the SE light beam was oriented orthogonally to the features to be measured. The measurements were carried out using the same library in use for production line monitoring and feedback-based Advanced Process Control (APC) specific to the post-development STI photo level under investigation.

Each wafer was inspected with a high density sampling of 736 points per wafer with 23 points per exposure field for a total of 5888 points, requiring a collection time of 160 minutes (average of 1.6s per point including wafer handling and alignment).

Figure 3 shows the wafer CD contour maps for the wafers covering the focus offsets from -90nm to +90nm. Note that minimum and maximum values for the color scale are the same for all maps. Observing the color gradients, it is evident that the CD range is changing its value with different focus excursions, with a minima lying at the best focus condition – a range between 0 and +30nm.

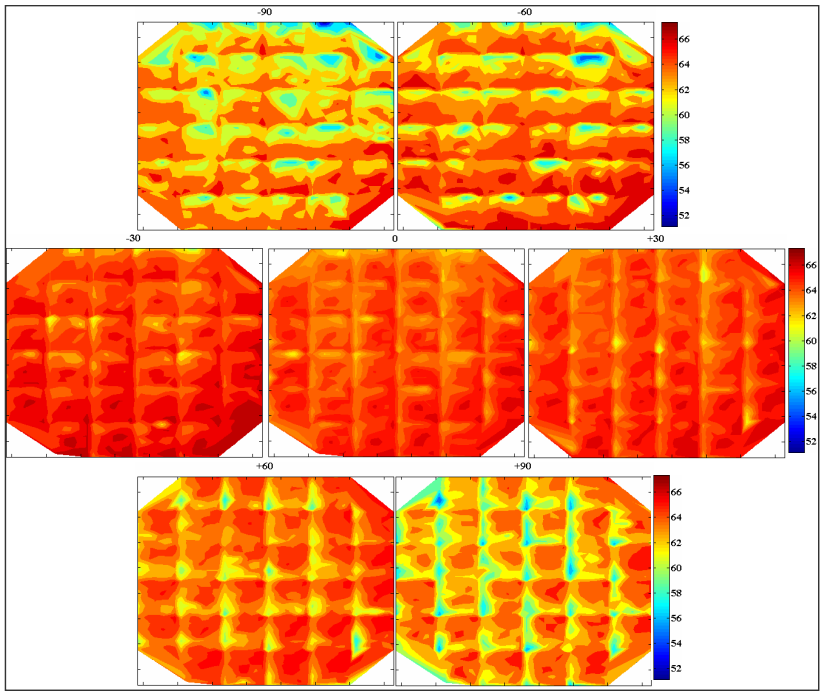

Fig. 3. CD maps from a Spectra CD-XT spectroscopic CD measurement tool for wafers with focus offsets ranging from -90nm to +90nm. Color bars are scaled on the same range for each map, with the maximum range of 20nm found on the wafer exposed at -90nm, the worst defocus condition.

The chart shown in Figure 4 shows that the distribution of average CD values for each wafer (blue line) lies on a hollow parabola (black line representing curve fit to the data). This is the typical pattern for a dense line printed feature when a defocus is applied; following the well-known Bossung curve behavior[3]. The parabola vertex is positioned at the nominal best focus condition, which for this wafer set is zero defocus. Error bars were set according to the following sigma precision calculation:

$$\sigma_{\text{Precision}} = \sqrt{\sigma_{\text{Short-term Repeatability}}^{2} + \sigma_{\text{Long-term Reproducibility}}^{2}}$$

This calculation is based on data collected for production metrology release of the SCD based APC loop for the level under investigation, leading to a value of +/- 0.5nm for CD of resist line measured at 50% of the profile height[4].

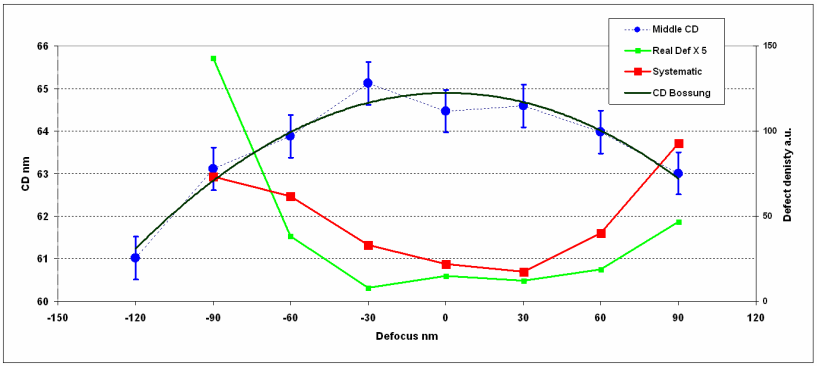

Fig. 4. Experimental Bossung plot shown versus defect density plotted in arbitrary units (a.u.).

When these CD values are compared to the systematic defect density (red curve in Figure 4), similar behavior is observed due to the fact that the best exposure conditions are chosen to guarantee that the lowest wafer CD range reaches the desired CD target with the lowest defect density specific to the STI photo layer (i.e. STI mask reticle).

Further exploring the metrology versus defect density correlation, it appears that the condition ensuring overall minimum systematic defect density is shifted +30nm relative to the zero defocus condition. The SCD measurement for the same defocus conditions shows that the points in the +30nm to -30nm range appear to be less well fit than the others and in a border-line condition with respect to ideal parabolic shape. Therefore the "uncertainty region" spans a defocus interval that may be compatible with systematic defect minimal density shift with respect to best focus assessment.

The meaning of these deviations may lie in the intrinsic, non-repeatable nature of the process used to determine absolute focus for the exposure system. This non-repeatability results in inaccuracies of the defocus value when setting focus around a zero defocus value. The error may descend from many parameters involved in the pattern imaging process, including systematic focus bias between scanner stages or substrate dependent variables such as local reflectivity variations that are well known to represent critical figures of merit in hyper-NA immersion lithography[4]. In order to determine the origin of these fine structures, a printing reproducibility experiment should be carried out as part of a future investigation. For example, this same analysis can be run on a set of wafers where the exposure process is iterated 10 times, thereby producing eight subsets of 10 wafers, each exposed at a different focus latitude.

The last step in the analysis was to quantify the extensions in terms of tolerable defocus of the 'no variation', 'CD variation', and 'defect printing' regions shown in Figures 2a and b. Figure 5 shows the exposure field signature of the intra-field CD dispersion compared to the defect distribution of the center wafer fields for wafers exposed at offsets of -90nm, 0nm and +90nm. This comparison demonstrates how measured CD variations can be correlated to defect detection.

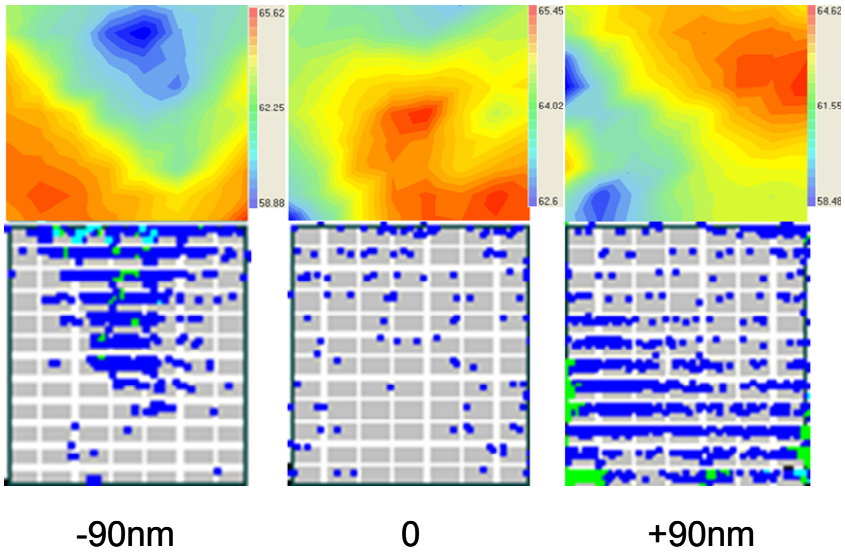

Fig. 5. Intrafield CD contour maps generated using a Spectra CD-XT compared to defect maps from the Puma 9000 for the center fields of the wafers exposed at -90nm, 0 and +90nm. Note the larger color scale range at the -90nm and +90nm conditions.

At best focus, the intra-field CD range is about 2.85nm. The assumption is that this is a residual of the mask reticle fingerprint. In this range, the CD deviation is not detected as systematic defects. At the opposite sides of the focus curve, the residual fingerprint is not present and a small CD is detected as systematic defects. In this range, physical random defects also start to print. The location of both types of defects overlapped to the intra-field CD map and defect-free areas correspond to CD values around 65nm – the target value on which the whole exposure process is tuned. The value of 65nm represents the baseline ideal target on which the darkfield imaging inspector recipe baseline was optimized.

2.3 Advanced ADI production data

The Puma 9000 darkfield imaging inspector was implemented in production for ADI for all 65nm flash devices for STI, poly, and line 1 photo layers. Over 10 months of production data (Figure 6), several excursions were detected, enabling defect engineers to quickly identify excursions related to litho tool focus drift, thereby preventing the printing of defocus-related defects on production wafers.

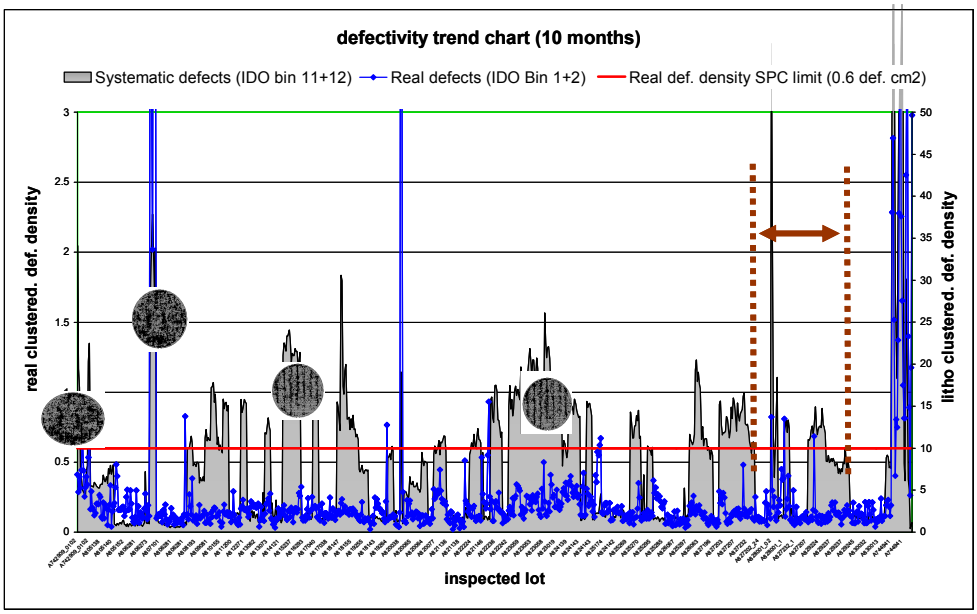

Fig. 6. Trend chart showing 10 months of production data from a 65nm flash STI ADI layer collected using the Puma 9000 darkfield imaging inspector with advanced defect binning. The grey solid bars represent the systematic defect density and the blue line represents random defect density. The red horizontal line represents the SPC limit for random defect density.

Figure 7 shows a sub-set of the 10 months of production data – the two months of data indicated by the vertical dashed lines in Figure 6. This data shows three possible excursions:

1. There is a very high increase in both the systematic and random defect density for several wafers. Representative defects include a large number of collapsed and lifted lines, shorts and large CD variations. As a result of this excursion, the litho equipment was taken off-line for re-qualification.
2. There is an increase in systematic defect density, and the random defect density is near the SPC limits. Wafer maps show a stepper field signature. Defects detected include shorts, modifications of critical structures and CD line variations. This excursion resulted in a warning being sent to the litho equipment engineers.
3. There is an increase in random defect density, but no increase in systematic defect density. This excursion is not related to focus drift.

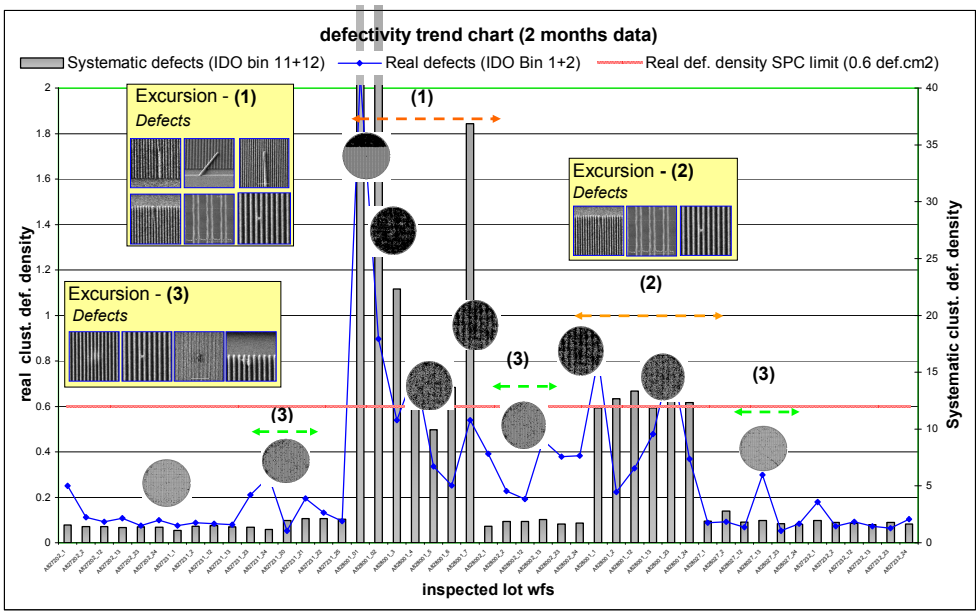

Fig. 7. Trend chart showing two months of production data from a 65nm flash STI ADI layer collected using the Puma 9000 darkfield imaging inspector with advanced defect binning. The grey solid bars represent the systematic defect density, the blue line represents random defect density, and the red horizontal line represents the SPC limit for random defect density. Three different types of excursions are highlighted.

This trend data validates the use of the darkfield imaging inspector for high-throughput production monitoring at ADI. With advanced binning capability, the darkfield imaging inspector allows engineers to monitor both random defectivity within the litho cell, and systematic defectivity that relates to focus issues. This inspection methodology is effective at detecting excursions and alerting engineers to out-of-focus situations, reducing the time required for scanner re-qualification and preventing yield-limiting defects from printing on production wafers.

3. ADVANCED PM FOR IMMERSION LITHOGRAPHY USING DARKFIELD IMAGING INSPECTOR

In addition to ADI applications within a dry litho cell, the Puma 9000 darkfield imaging inspector with advanced binning capability has proven effective as a photo-cell monitor (PM) for immersion lithography production. By increasing the effective numerical aperture (NA) of the imaging lens, immersion lithography enables the printing of smaller design rules at higher yields with a better process window than equivalent dry systems. Immersion lithography is a key technology for sub-65nm device patterning, but defect reduction for immersion lithography remains a challenge for chipmakers. When compared to dry lithography defects, the defect populations that occur on immersion-exposed photoresists arise from different mechanisms and display different wafer distributions. Immersion lithography defect types and mechanisms have been well-documented[5, 6, 7, 8, 9].

PM is a key component of an immersion lithography defect reduction strategy, helping engineers to identify defect sources during ramp-up and sub-system failures during production. This section describes immersion lithography PM applications, the investigation of different inspection technologies for use in these PM applications, and the implementation of a darkfield imaging inspector within the immersion lithography cell.

3.1 PM applications and requirements

Photo-cell monitoring (PM) is a well-established technique for qualifying and monitoring track and scanner performance. PM uses test wafers patterned with either a device layer reticle or a test reticle. The wafers are processed and then inspected on a patterned wafer inspector in order to identify litho-related defects and help optimize litho process conditions. Broadband brightfield inspectors are traditionally used for PM because the tools utilize selectable

illumination bands and optical apertures to produce the highest sensitivity to litho DOI[1, 8, 9, 10, 11]. The number of PM inspections performed can be limited by the brightfield inspector's throughput and the associated costs of PM (for example, track downtime and test wafer cost). On average, 100 – 200 wafers per week are used for PM for a ~6k WSPW fab.

Typical immersion lithography PM applications and their associated inspection requirements are shown in Table 1. Applications such as immersion lithography qualification, process development and incoming resist qualification use broadband brightfield inspectors to produce the required high sensitivity inspections and high capture rates of critical litho DOI. The inspection sensitivity requirements for production monitoring are less stringent, and thus, this application is a good target for moving from brightfield to a different inspector. The Puma 9000 darkfield imaging inspector with advanced binning capability has demonstrated sensitivity to litho DOI, providing a high throughput option for litho defect monitoring[2]. As such, an investigation was done to compare relative capture of critical immersion litho defects among different inspectors. The focus of this evaluation was to determine if the darkfield imaging tool could be implemented for immersion lithography daily PM, thereby freeing the brightfield inspector for additional tasks.

Table 1. Typical immersion lithography PM applications.

Application	Objective	Inspection Requirement	Target Inspector: Required Sensitivity at Lowest CoO
Immersion lithography ramp-up	De-bug; defect reduction; benchmark with dry litho or other immersion litho	Highest sensitivity and capture rate of critical litho DOI	DUV Broadband Brightfield
New resist development and/or qualification	Select base resist and integrate in process	Highest sensitivity and capture rate of critical litho DOI	DUV Broadband Brightfield
Production: daily monitor	Monitor possible litho excursions	High capture rate of critical DOI at high throughput	Darkfield Imaging

3.2 Immersion lithography PM: inspector comparison

The evaluation for determining the best tool to use as an immersion litho daily monitor utilized two STI NOR flash litho layers – 65nm and 45nm. Three inspectors were included in the evaluation: the 2800 DUV broadband brightfield inspector, the Puma 9000 darkfield imaging inspector, and the AIT XP traditional darkfield inspector. The goal of the evaluation was to determine if a darkfield inspector provided good enough sensitivity to detect litho excursions, at a lower CoO, thereby freeing brightfield inspector tool capacity for litho development work.

Data analysis was performed and validated on four lots for both STI layers. The sensitivity goal was to maintain >75% capture on DOI compared to the most sensitive inspector. Figure 8 shows an example of a Pareto obtained as part of this detailed evaluation.

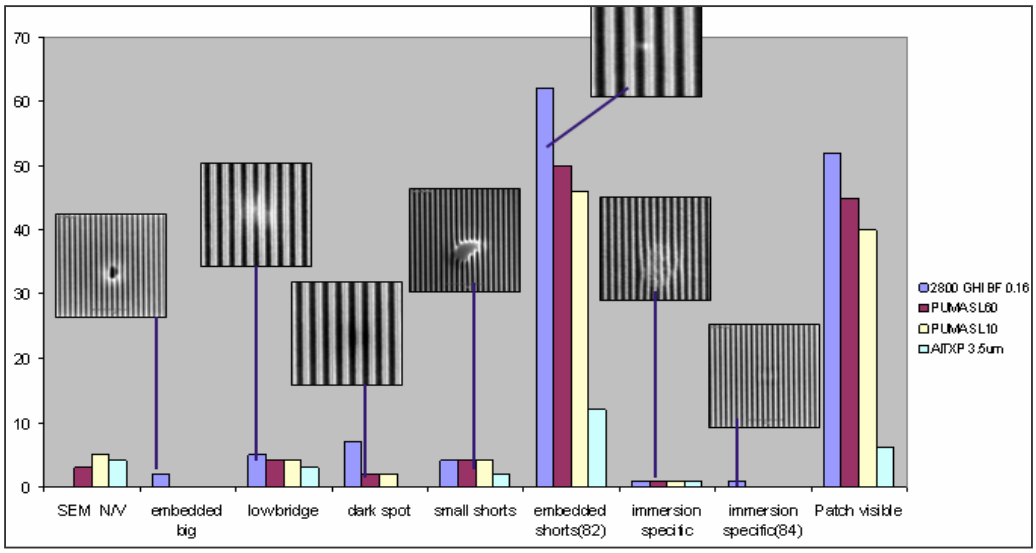

Fig. 8. Defect Pareto comparing inspection results from a 45nm STI litho layer. The inspectors evaluated include: 2800 broadband brightfield inspector, Puma 9000 darkfield imaging inspector (at two different sensitivity settings) and AIT XP traditional darkfield inspector.

Table 2 summarizes the results of the investigation. The analysis showed that the darkfield imaging inspector provided good sensitivity to litho defects at high throughput, and had a very low risk of missing litho excursions. As such, it was determined that the darkfield imaging inspector should be implemented as the tool-of-record for immersion lithography daily PM. The broadband brightfield inspector provided the best sensitivity to litho DOI and should continue to be used for all litho engineering activities and for detailed investigation of immersion lithography defect and process issues.

Table 2. Inspector evaluation results for immersion lithography daily PM.

Inspector	**Pixel Size**	**Throughput** (wafers per hour)	**Sensitivity** (Average DOI capture %)	**Daily Tool Loading %** (at 6 wafers per day)	**Conclusions**
2800	0.16µm	Low	100%	25%	• Best sensitivity • Heavy tool loading • Use as baseline, sensitivity standard
Puma 9000	**sL60**	**High**	**83%**	**1.9%**	**• Good sensitivity** **• Acceptable tool loading** **• Good excursion detection**
Puma 9000	sL10	Very High	73%	0.8%	• Good enough sensitivity • Very low tool loading • Good enough excursion detection
AIT XP	3.5µm	Medium	21%	1.2%	• Very low sensitivity • Low tool loading • High risk to miss excursions

3.3 Immersion lithography PM implementation: advanced defect binning

An additional step in the implementation of the darkfield imaging inspector for immersion lithography daily PM was to establish automated defect binning as part of the inspection. Software integrated on the Puma 9000 inspector allows defects to be automatically sorted into different rough bins. This binning data is integrated with the fab automation, and an immersion litho tool can be stopped in real-time if an excursion is detected.

The defect bins set up on the darkfield imaging inspector were based on defect size, and resulted in the immersion litho defect populations being grouped into three main classes. These defect classes are shown in Figure 9.

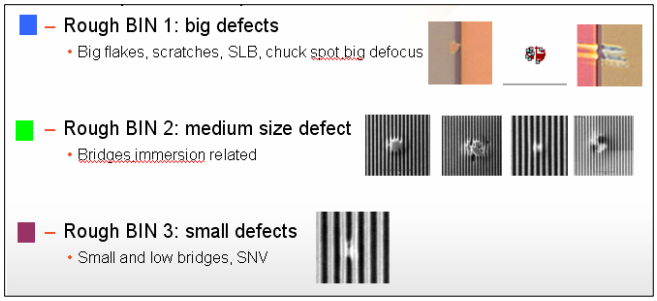

Fig. 9. Rough bin scheme set up using the iDO (inline Defect Organizer) automatic defect binning feature on the Puma 9000 darkfield imaging inspector. Immersion litho defects are separated into three different defect bins based on size.

Excursions for these rough bins were related to different litho issues. For example, an increase in the number of defects in rough bin 1 correlated to a super large bubble (SLB) defect excursion. In order to provide the information necessary to identify the root cause of an excursion, 50 high resolution images are captured for defects in rough bins 1 and 2 when an excursion is detected. When a rough bin 3 excursion occurs, the wafer is sent directly to SEM for further analysis. Figure 10 shows a defect density trend chart for daily monitoring using the darkfield imaging inspector with automated defect binning. This chart shows three different excursions that are well-correlated with different rough bin defect density excursions. Overall, the darkfield imaging inspector has proven to be an effective tool for immersion lithography daily PM.

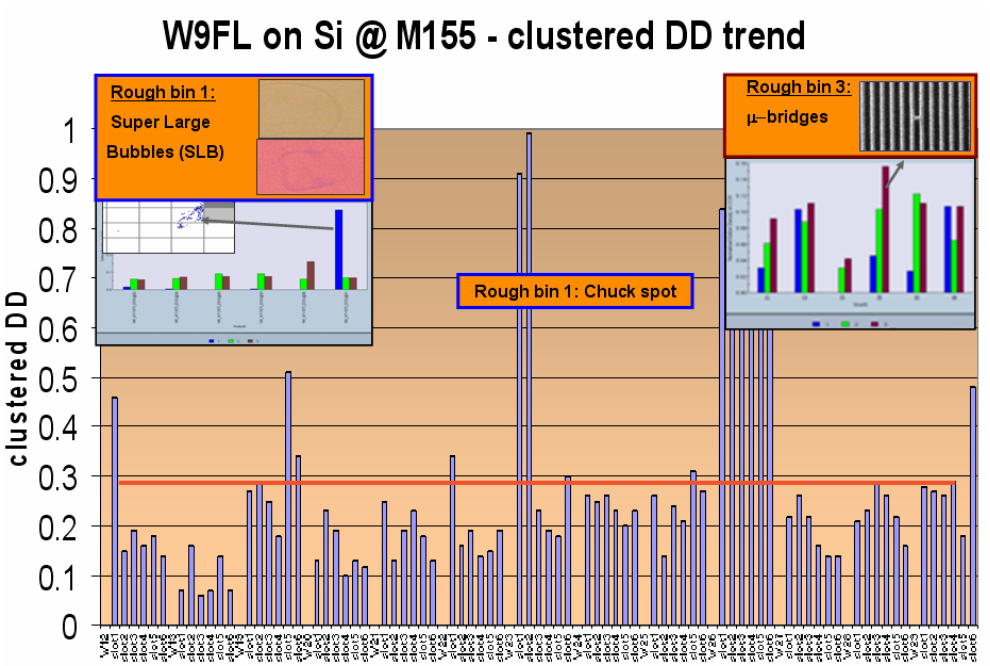

Fig. 10. Example of a PM defect density trend chart. Three types of excursions are shown, each related to an increase in defect density in a particular rough bin, and each related to a specific immersion litho defect excursion (SLB, chuck spot and micro-bridges).

4. CONCLUSIONS

A new inspection methodology utilizing the Puma 9000 darkfield imaging inspector has been implemented for ADI and PM at 65nm and 45nm. A very high sensitivity inspection is used in conjunction with advanced defect binning to monitor defect and process excursions within the litho cell.

For ADI, this inspection methodology allowed engineers to monitor 'color variation' defects that corresponded to CD variations on the wafer. An extensive study using a set of wafers exposed at different focus offsets demonstrated the capability of the darkfield imaging inspector with advanced binning to effectively detect focus excursions. The defect results correlated well with spectroscopic CD measurements performed on the wafers. In addition, 10 months of production data showed that this inspection technique could successfully detect both random excursions within the litho cell, and systematic defect excursions that allowed engineers to take preventative action before a defocus condition resulted in printed defects on the wafers.

For PM, this inspection methodology produced good sensitivity to immersion-litho defects at a lower cost-of-ownership. The darkfield imaging inspector was implemented as a daily PM for the immersion lithography cell. Production data using defect binning demonstrated several excursions – each well correlated to an increase in a defect bin that related to a specific immersion-litho defect type.

This novel inspection methodology has proven to be a critical component in the litho cell excursion monitoring strategy at Numonyx. This novel inspection methodology is extendible to other layers and design rules and should be considered when exploring techniques for detecting CD variations, subtle immersion-litho, or other low signal-to-noise defects.

REFERENCES

[1] Chen, Z.Y., Chou, I.C., Yang, J.H., Chen, W., Chang, J., Chen, H., Ng, M., Perry-Sullivan, C., and Li, M., "Advanced technology for after-develop inspection," Proc. SPIE 7140, 71400Y (2008).

[2] Mäge, I., Seifert, U., Saville, B., and Tuckermann, M., "Developing micro ADI methodology for new litho process monitoring strategies," Semiconductor Fabtech, 36th Edition (2007).

[3] Ausschnitt, C.P., and Brunner, T.A., "Distinguishing dose, focus and blur for lithography characterization and control," Proc. SPIE 6520, 65200M (2007).

[4] Loi, S., Fasciszewski Zeballos, A., Iessi, U., Robinson, J., Izikson, P., Mani, A., and Polli, M., "In-line focus-dose monitoring for hyper NA imaging," Proc. SPIE 6922, 69223H (2008).

[5] Malik, I., and Pinto, B., "Immersion Changes Litho Cluster Qualification," Semiconductor International (2006).

[6] Warrick, S., Cruau, D., Mauri, A., Farys, V., and Gaugiran, S., "A defectivity checkpoint for immersion lithography," Microlithography World (2006).

[7] Wei, Y., Brandl, S., Goodwin, F., and Back, D., "193nm Immersion-Related Defects and Strategies of Defect Reduction," Future Fab International, Issue 22 (2007).

[8] Malik, I., and Nag, S., "Defectivity Challenges in Immersion Lithography for sub-90nm Technologies," Lithography Users Forum (2006).

[9] Kocsis, M., et al, "Immersion specific defect mechanisms: findings and recommendations for their control," Proc. SPIE 6154, 615409 (2006).

[10] Lee, H., Leong, C., Yik, J., Lim, V., Hong, G.F., Chia, W., and Liu, D., "Qualification and Monitoring of Immersion Lithography Process for 45nm Development", Yield Management Seminar (2007).

[11] Perry-Sullivan, C., Le Roy, E., Lange, S., Malik, I., Yerabaka, A., Wilson, A., Shirey, M., and Pinto, B., "Broadband Brightfield Inspection Enables Advanced Immersion Lithography Defect Detection," Yield Management Solutions (2007).